

Observation of large- D magnetic phase in $\text{Sr}_3\text{NiPtO}_6$

S. Chattopadhyay,¹ Deepti Jain,² V. Ganesan,² S. Giri,¹ and S. Majumdar^{1,*}

¹*Department of Solid State Physics, Indian Association for the Cultivation of Science, 2A & B Raja S. C. Mullick Road, Kolkata 700 032, India*

²*UGC-DAE Consortium for Scientific Research, University Campus, Khandwa Road, Indore 452 017, India*
(Received 31 May 2010; revised manuscript received 15 July 2010; published 17 September 2010)

We report the magnetic and heat-capacity measurements on the single-crystalline sample of $\text{Sr}_3\text{NiPtO}_6$, an $S=1$ spin-chain compound. Previous studies on the compound indicated a nonmagnetic ground state with large single-ion anisotropy. We observe the presence of short-range spin-spin correlation in our susceptibility and heat-capacity data. The system shows a magnetically disordered ground state below 10 K with the signature of finite gap in the spin-excitation spectra. The low-lying excitation of the system, both obtained from heat capacity and the susceptibility data, corresponds well with the exciton model for large- D phase as observed in few other one-dimensional integer spin systems where anisotropy exceeds the spin-spin exchange interaction.

DOI: [10.1103/PhysRevB.82.094431](https://doi.org/10.1103/PhysRevB.82.094431)

PACS number(s): 75.45.+j, 75.10.Pq, 75.30.Gw, 75.40.Cx

I. INTRODUCTION

$S=1$ spin-chain compounds with Heisenberg antiferromagnetic (HAFM) exchange interaction (J) have attracted huge attention mainly due to the existence of Haldane gap.¹⁻³ Presence of single-ion anisotropy along with J turns this $S=1$ family more fascinating because of the rich phase diagram which results from the interplay between these two competing interactions. In presence of planar anisotropy, the spin part of the Hamiltonian of a single isolated chain can be written as

$$\mathcal{H}_{spin} = -J \sum_{i=1}^N \vec{S}_i \cdot \vec{S}_{i+1} + D \sum_{i=1}^N (S_{iz})^2 - \tilde{g} \mu_B \sum_{i=1}^N \vec{H} \cdot \vec{S}_i \quad (1)$$

The first term is the isotropic Heisenberg exchange interaction term with nearest neighbor intrachain interaction while the second term accounts for the planar anisotropy ($D \geq 0$) along z axis and the last term corresponds to the effect of applied magnetic field (H). Here, \tilde{g} is the Landé g -factor tensor, μ_B is the Bohr magneton, and N is the number of spins on the chain. A wealth of theoretical studies have been performed on systems represented by the above Hamiltonian, and it has been found that the anisotropy to exchange ratio D/J controls the quantum fluctuations and stabilizes different phases.^{4,5} The well-known Haldane phase persists in the range $-0.25 \leq D/|J| < 0.97$ (Refs. 6 and 7) with a characteristic spin gap (referred as Haldane gap) between nonmagnetic ground state and lowest excited state. The Haldane gap vanishes at the critical value of $(D/|J|)_c = 0.97$. However, with further increase in the ratio, the gap reopens, but the origin is dominated by the large value of D . Such gapped phase is distinctively different from the Haldane phase, and this region with $D/|J| > 1$ is known as “large- D ” (LD) phase.^{4,5,7-10} This phase is characterized by a *unique disordered magnetic ground state* with a gap in the spin-excitation spectra.

The basic difference between an LD and a Haldane phase is that the later is associated with some hidden short-range AFM order (the so called string order, $\mathcal{O}_{string}^\alpha$ being nonzero) while the former does not show any degrees of order

($\mathcal{O}_{string}^\alpha = 0$).¹¹ As a result the Haldane phase is often termed as a spin-liquid phase as opposed to the “gas” phase at large D . In the extreme limit ($D/|J| \rightarrow \infty$), the ground state of the LD phase is represented by vanishing azimuthal spin components at each site ($S_z^i = 0$ for $i=1$ to N). However, for finite value of $D/|J|$ (i.e., the case of LD phase), S_z^i can attain value $+1$ or -1 at some sites. These $+1$ and -1 spin sites are spatially uncorrelated and mobile as gas particles. The lowest excited state of the LD phase is the formation of $+1$ and -1 bound pairs in presence of finite spin-spin correlation along the azimuthal direction and it can be identified from its unique low-lying excitation.

Despite immense theoretical and experimental works in the last two decades, understanding the physics of such weakly coupled integer spin-chain systems is still a fertile ground for research. They can exhibit interesting magnetic ground states along with unusual spin excitation spectra, such as Haldane, LD, XY1, XY2, Néel phases, etc.⁵ However, other than Haldane phase, very little work has been performed to identify these exotic phases in real materials. An example of the novelty of such quantum spin systems is the recent discovery of Bose-Einstein condensation (BEC) of spin degrees of freedom in $\text{NiCl}_2\text{-4SC(NH}_2)_2$ (DTN, an $S=1$ compound with planar anisotropy),¹²⁻¹⁴ where a field-induced magnetic ordering is interpreted as BEC of magnons. Also, in LD phase compound $\text{Ni(C}_2\text{H}_8\text{N}_2)_2\text{Ni(CN)}_4$ (NENC) existence of single-ion bound states were observed.^{15,16} Such exotic features affirm the relevance of research in similar integer spin systems. So far, the LD phase is predicted only in few real materials, such as NENC, DTN, $\text{Ni(C}_{10}\text{H}_8\text{N}_2)_2\text{Ni(CN)}_4 \cdot \text{H}_2\text{O}$, CsFeBr_3 ,^{6,12,17,18} etc. The title compound of the present work, $\text{Sr}_3\text{NiPtO}_6$ (SNPO) is also a $S=1$ chain system with large planar anisotropy arising from single-ion effect ($D \sim 94$ K),¹⁹ and among inorganic oxides, it is a strong candidate for the LD phase.

SNPO belongs to the family of quasi-one-dimensional (1D) oxides with K_4CdCl_6 type crystal structure. In this system Pt^{+4} and Ni^{+2} occupy the octahedral and trigonal prismatic sites respectively making PtO_6 and NiO_6 environments as shown in detail in Fig. 1. Due to the low spin configuration, Pt^{+4} has zero effective moment here. Ni^{+2} ions are the

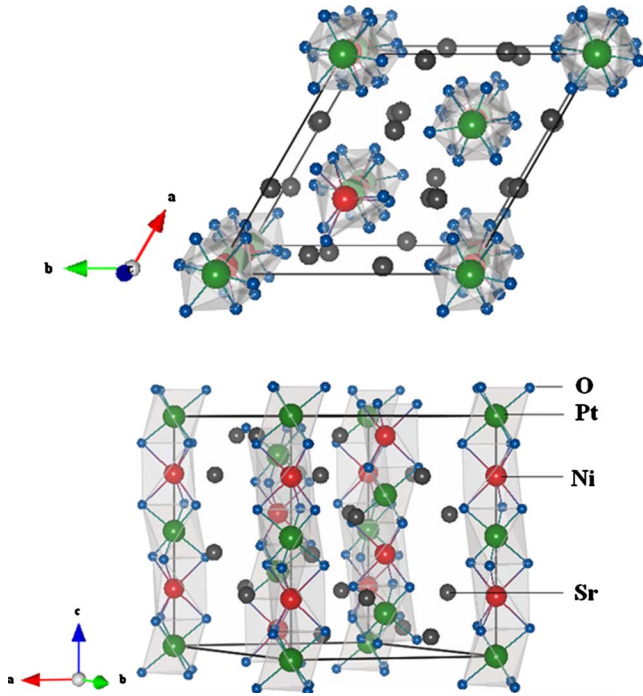


FIG. 1. (Color online) The upper panel shows a perspective view of a unit cell of SNPO seen along the c axis, whereas bottom panel shows $-\text{Ni-Pt-Ni-Pt}-$ chains as an array of alternating (Pt) and (Ni) ions. PtO_6 octahedra and NiO_6 trigonal prisms can be seen as a series of gray blocks where oxygen atoms are indicated by small blue spheres. In the left side arrows indicate the directions of the basis vectors.

only magnetic species present in this system forming an alternating chain ($-\text{Ni-Pt-Ni-Pt}-$) along the crystallographic c axis (or the z axis of the spin Hamiltonian). Being a quasi-1D $S=1$ HAFM compound with large D , it can be a good candidate for the LD phase. Although, the SNPO has been studied previously both in the single-crystalline^{19,20} and polycrystalline²¹ forms, information regarding the true nature of the magnetic ground state is still lacking. The main objective of the present work is to understand the ground-state magnetic properties of this very interesting composition through careful magnetic and heat-capacity measurements on single-crystalline sample. Our result conclusively establishes the fact that the material indeed shows all the properties expected for an LD phase.

II. EXPERIMENTAL DETAILS

Single crystals of SNPO were grown using flux method as described by Claridge *et al.*¹⁹ The average length of the rod-shaped crystals were few mm. The x-ray powder-diffraction pattern at room temperature was recorded in a Bruker axis D8 advanced diffractometer using $\text{Cu } K_\alpha$ radiation by crushing few crystals. It clearly indicates that the sample is single phase in nature. SNPO belongs to trigonal crystal system with space group $R\bar{3}C$. From the diffraction data, the calculated lattice parameters are found to be $a=9.55 \text{ \AA}$ and $c=11.16 \text{ \AA}$, which are very close to the previously reported

values.¹⁹ To ensure the crystal quality and to find out the crystallographic orientation, Laue diffraction was performed. It ensured the high quality of the crystals and from the Laue analysis, the rod axis was identified as c axis. Magnetization (M) measurement from 2 to 300 K was performed along and perpendicular to the c axis using a single piece of SNPO crystal on a Quantum Design magnetic property measurement system. Heat-capacity (C) measurement was carried out using a Quantum Design physical property measurement system.

III. RESULTS AND ANALYSES

A. Magnetization

In case of a spin-chain compound, the total measured susceptibility ($\chi=M/H$) is often expressed as the combination of different contributions

$$\chi = \chi_o + \chi_{curie} + \chi_{spin}, \quad (2)$$

where, χ_o is a T -independent term originating from core diamagnetism, van Vleck paramagnetism and other external effects. The term $\chi_{curie} = C/(T-\theta)$ is the Curie-type contribution appears due to paramagnetic impurity and/or broken-chain effect, and a common manifestation of this term is the presence of low- T up turn in χ .²² All other contributions arising from the spins at the lattice sites are incorporated in the intrinsic part χ_{spin} . We measured T variation in χ along and perpendicular to the c axis (denoted by χ^{\parallel} and χ^{\perp} , respectively). Strong anisotropy is observed in the measured susceptibility in two orthogonal directions, which was already observed by Claridge *et al.*¹⁹ The observed anisotropy was found to be related to the single-ion anisotropy associated with the Ni^{2+} ions, which forces the spins to lie in the ab plane [see the cartoon in Fig. 2(b)].

In order to understand the magnetic state of the sample, one needs to separate out the intrinsic contribution χ_{spin} . For the present sample, χ_{spin} was estimated by subtracting the combined effect of χ_o and χ_{curie} from the total measured susceptibility. The fitting of the $\chi^{\parallel}(T)$ data at low- T (below 4 K, where χ_{spin} is small) to $\chi_{curie} + \chi_o$ produced $\chi_o = -7 \times 10^{-4} \text{ emu/mol}$, the extrinsic Curie constant, $C = 0.03 \text{ emu K/mol}$ and $\theta = -4.52 \text{ K}$. Subtracting the contribution of χ_o and χ_{curie} from χ^{\parallel} and χ^{\perp} , we obtained the χ_{spin} contributions, which have been depicted in Fig. 2(a). The anisotropy is quite clearly visible with χ_{spin}^{\parallel} being higher in magnitude than χ_{spin}^{\perp} . In addition, they also differ in nature. While, χ_{spin}^{\perp} shows a monotonic increase followed by a saturating tendency below 10 K with decreasing T , χ_{spin}^{\parallel} shows a peak around 60 K followed by an exponential drop with further decrease in T , which is a typical signature of zero-field splitting in presence of D . Most interestingly, χ_{spin}^{\parallel} shows a flat region with almost zero magnitude below 10 K [see inset of Fig. 2(a)]. Such feature indicates an unusual nonmagnetic ground state with effective zero magnetic moment in SNPO.

Considering such low- T anomaly, we carefully investigated the region below 50 K. In Fig. 2(b), we have shown the field-cooled (FC) and zero-field-cooled (ZFC) susceptibili-

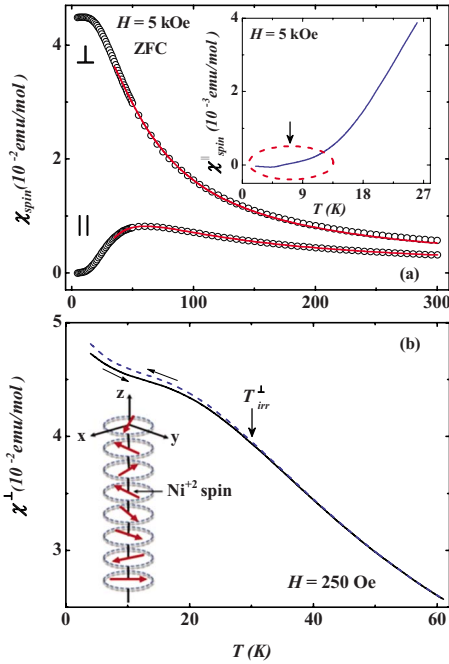


FIG. 2. (Color online) (a) shows the temperature variation in spin susceptibility (χ_{spin}) measured along and perpendicular to the c axis. The solid lines show fitting to the data using single ion anisotropy model (see text). The inset shows an enlarged view of the low temperature χ_{spin} for the parallel direction. (b) shows the zero-field-cooled and field-cooled susceptibility measured perpendicular to the c axis. The inset shows a cartoon of the possible ground state spin structure for $D/|J| \rightarrow \infty$ with all the spins lying in the ab plane (denoted by circles).

ties in presence of $H=250$ Oe measured perpendicular to the chain direction, which is the easy plane for magnetization in presence of D . A clear bifurcation between FC and ZFC data takes place at $T_{irr}^{\perp}=30$ K, which is not expected for isolated Ni^{2+} ions. Such bifurcation can happen if there is some finite spin-spin correlation in the system, whether it be long range, short range or glassy in nature. Long-range magnetic order can be ruled out for the present sample, which is supported by the absence of any anomaly in the heat-capacity data discussed later. In this series of materials (general formula A_3XYO_6) various magnetic phenomena are related to finite J . The Cu counterpart, namely, Sr_3CuPtO_6 (SCPO) with very similar crystal structure has J close to -26 K.²³ The complex nature of the magnetic susceptibility including irreversibility in the FC and ZFC data at low- T in SNPO indicates the existence of finite J .

It becomes apparent that a simple model for single-ion anisotropy is inadequate to explain the magnetic ground state of SNPO and the presence of J is expected to modify overall susceptibility of the system. In the previous analysis, Claridge *et al.*¹⁹ fitted the χ data with the model solely based on single ion anisotropy ($J=0$) (Refs. 24 and 25) in a limited T range and obtained $D=93.7$ K. The fit deviates significantly below 40 K, particularly in the parallel direction. We fitted our χ_{spin} data with the same model for single ion anisotropy, however, failed to get a good fit between 35 and 300 K for a single value of D for both the directions. Allowing D to be

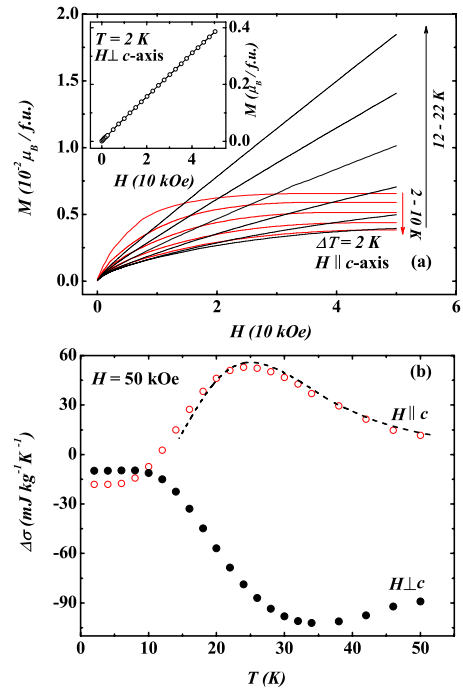


FIG. 3. (Color online) (a) depicts the isothermal magnetization curves measured parallel to the c axis between 2 and 22 K. The inset shows the magnetization curve measured perpendicular to the c -axis at 2 K. (b) shows the change in magnetic entropy by the change in magnetic field from 0 to 50 kOe measured for both parallel ($\Delta\sigma^{\parallel}$) and perpendicular ($\Delta\sigma^{\perp}$) directions. Dashed line is the simulated data of $\Delta\sigma^{\parallel}$ using the strong coupling relation of χ_{spin}^{\parallel} .

anisotropic (*i.e.*, different in parallel and perpendicular directions), we obtained reasonably good fit between 35 and 300 K (above the low- T region of anomaly), which has been shown by solid lines in Fig. 2(a). The anisotropy in D is found to exist in different sets of data measured at different fields (250 Oe, 2 kOe, and 5 kOe) and even on crystals obtained from different batches. The magnitude of D (in both directions) is found to vary slightly with H (maximum 3%). At $H=5$ kOe, we obtained $D=88.65$ K and 107.47 K along and perpendicular to the chain directions, respectively, and the corresponding g -factors are $g^{\parallel}=2.04$ and $g^{\perp}=2.44$. The average value of D and also the values of g are found to be in close agreement with the previous data.¹⁹ Such anisotropy in D is not acceptable in the model for single-ion anisotropy and it arises from the influence of J on D , which continues to exist even at high- T . The observed anisotropy in D is an artifact of the model used for a system where D and J are both present. Similar anisotropic D was observed in NENC, where poor quality of fittings in parallel and perpendicular directions were considerably improved by choosing anisotropic values of the fitting parameters.¹⁶

The ground-state magnetic properties of SNPO were further probed by isothermal magnetization measurements at different constant temperatures [Fig. 3(a)]. For $H \perp c$, M - H curves are perfectly linear for all the temperature of measurements (between 2 and 50 K). On the other hand, M measured \parallel to c axis shows anomalous behavior. At very low- T (between 2 and 10 K), M shows prominent signature of a plateaulike region, with very small value of the moment. How-

ever, above 10 K, M enhances and shows a linear M - H behavior.

It might be interesting to see the change in magnetic entropy ($\Delta\sigma$) under an applied field H , which is generally a measure of the magnetocaloric effect (MCE) of a sample. Here, $\Delta\sigma$ was calculated in both of the directions from M - H data collected at varied T using the relation

$$\Delta\sigma(0 \rightarrow H') = \int_0^{H'} \left(\frac{\partial M}{\partial T} \right)_H dH. \quad (3)$$

Figure 3(b) describes T variation (between 2 and 50 K) of $\Delta\sigma$ along ($\Delta\sigma^{\parallel}$) and perpendicular ($\Delta\sigma^{\perp}$) to the c axis for H changing from 0 to 50 kOe. Interestingly, $\Delta\sigma$ is found to have different signs in two orthogonal directions. $\Delta\sigma^{\parallel}$ is found to be positive above 12 K and shows broad peaklike feature at around 24 K while $\Delta\sigma^{\perp}$ is negative in the whole measured T with a broad minimum around 34 K. The T variation in $\Delta\sigma$ in both the directions shows a prominent flat region below 10 K with magnitude close to zero. The observed sign of MCE is actually in accordance with the anisotropic spin arrangements as shown in the inset of Fig. 2(b). Due to the presence of planar anisotropy, the spins are free to rotate on the ab plane. When a magnetic field is applied perpendicular to the c axis, spins get aligned to the direction of H , and a negative $\Delta\sigma$ is observed. On the other hand, it is hard to rotate the spins considerably by applying H along c axis. Only a small positive $\Delta\sigma^{\parallel}$ is observed due to minute spin canting, which actually introduces magnetic disorder. So far, we have not taken into account any spin-spin correlations. But due to finite J , antiferromagnetically aligned domains will be formed at low temperatures, which will make the spins to be less sensitive to applied H , and consequently a decrease in the magnitude of $\Delta\sigma$ is noticed for both the directions with decreasing T . Below about 10 K, we notice that $\Delta\sigma$ is very small and almost independent of temperature. This actually corresponds to the disordered gaped phase as observed in the $M(H)$ and $\chi(T)$ measurements.

B. Heat capacity

Figure 4(a) displays T variation in C of SNPO (C_{SNPO}) between 2 and 100 K. It is clear that there is no signature of long-range ordering down to the lowest measured T . In order to extract the magnetic contribution of heat capacity (C_{mag}), it is essential to subtract the lattice part (C_{latt}) from the total C . To calculate C_{latt} of SNPO, we used the $C(T)$ data of the nonmagnetic isostructural compound $\text{Sr}_3\text{ZnPtO}_6$ (SZPO). Due to the mass difference between Ni and Zn, effective Debye temperatures of SNPO and SZPO will be different and proper scaling was performed to estimate the correct C_{latt} of SNPO.²⁶ It is clearly seen that C_{SNPO} is always greater than C_{latt} , which is due to the excess magnetic contribution in the Ni sample. At high T , C_{SNPO} is found to approach C_{latt} . The T variation in C_{mag} has been displayed in Fig. 4(b). $C_{\text{mag}}(T)$ shows a clear humplike feature close to 32 K. This typical feature signifies the existence of some short-range magnetic correlation. This is also in accordance with the observed deviation between FC and ZFC susceptibilities measured perpendicular to the chain direction.

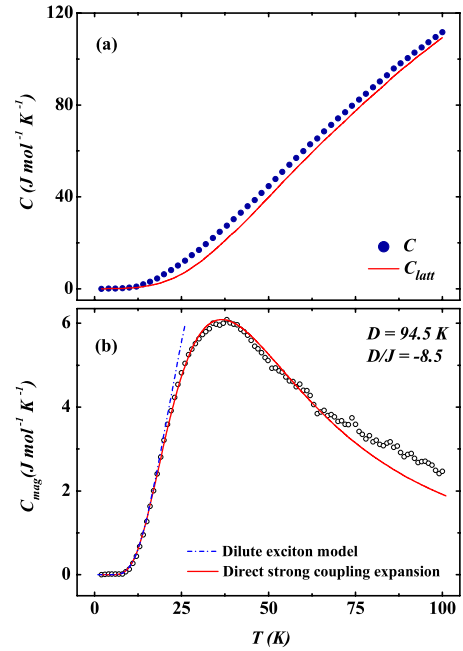


FIG. 4. (Color online) (a) Heat capacity as a function of temperature (below 100 K) for $\text{Sr}_3\text{NiPtO}_6$. The lattice contribution of the heat capacity (denoted by the solid line) is also shown in the figure, which has been obtained from the heat capacity data of $\text{Sr}_3\text{ZnPtO}_6$ by requisite scaling. (b) shows the magnetic contribution to the heat capacity of $\text{Sr}_3\text{NiPtO}_6$ along with the fittings by dilute exciton model (dashed line) and direct strong coupling expansion (solid line).

The most notable feature in C_{mag} is that it becomes zero at a finite temperature (at around 10 K), and forms a plateau-like region. This is in contrast with the isostructural $S = \frac{1}{2}$ compound SCPO, where $C_{\text{mag}}(T)$ shows a power-law behavior down to 2 K.²³ This anomaly in SNPO is also visible in some form in the $\chi(T)$ and $\Delta\sigma$ data as discussed above. Considering SNPO is an $S = 1$ system, such feature in the heat capacity and other measurements clearly indicate that there exists a gap in the spin excitation spectra. Very similar nature of C_{mag} (humplike feature followed by a plateau with almost zero magnitude) has been observed in case of NENC and it is attributed to a spin gap in the LD phase.⁶

C. Data analysis

From our study and previously published data, it is clear that the SNPO (i) has large D value which gives rise to planar anisotropy and (ii) it has finite intrachain spin-spin correlation present, which is responsible for the low- T anomaly. It is obvious that J will be smaller than D ($D/|J| > 1$) for the present sample because all the anomalies related to spin-spin correlation occur at least below 30 K while D is in the range of 100 K. Therefore, SNPO is found to be a good candidate for the LD phase and such LD state has been recently realized experimentally in NENC below 2 K.

In order to have a definite proof for the LD phase in SNPO, one needs to see whether the magnetic excitation spectra truly obey the expected dispersion relation. For LD

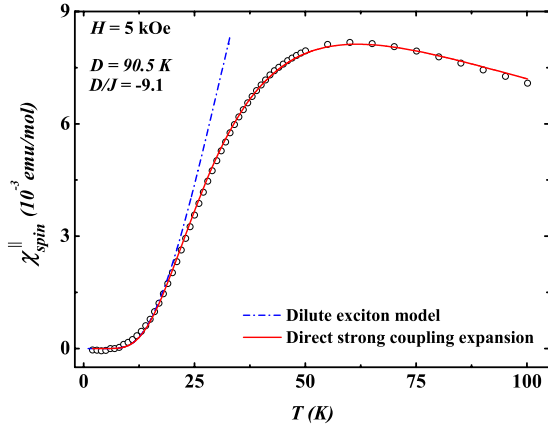


FIG. 5. (Color online) Spin contribution of the parallel susceptibility is plotted as a function of temperature. The dashed and the solid lines show fittings by dilute exciton model and direct strong coupling expansion, respectively.

systems, the $S_z=0$ ground state is separated by an energy gap from the lowest excited state having $S_z = \pm 1$ (known as exciton or antiexciton, respectively). Papanicolaou and Spathis^{27,28} formulated an energy-momentum dispersion relation for the excitonic (or antiexcitonic) mode given by

$$\omega(k) = D(1 + \omega_1/a + \omega_2/a^2 + \omega_3/a^3 + \dots) \quad (4)$$

Here $\omega(k)$ corresponds to the excitation energy, $a=D/J$, $\omega_1 = -2 \cos(k)$, $\omega_2 = 1 + 2 \sin^2(k)$, and $\omega_3 = \frac{1}{2}[1 + 8 \sin^2(k)]\cos(k) - 2 \sin^2(k)$ and so on for an isotropic HAFM system. Both ω and D are expressed in terms of temperature. If one further assumes that the excitons are mutually noninteracting (so called *dilute exciton* limit), it is possible to write down the expressions for the excitonic contribution of heat capacity and parallel susceptibility as^{6,29}

$$C_{exc}(T) = \frac{R}{\pi} \frac{d}{dT} \int_{-\pi}^{\pi} \frac{\omega(k) dk}{\exp[\omega(k)/T] - 1}, \quad (5)$$

$$\chi_{exc}^{\parallel}(T) = \frac{N_A g^2 \mu_B^2}{4\pi k_B T} \int_{-\pi}^{\pi} \frac{dk}{\sinh^2 \left[\frac{\omega(k)}{2T} \right]}. \quad (6)$$

Here N_A , R , and k_B , are respectively Avogadro's number, universal gas constant and Boltzmann constant. It should be noted that such model for noninteracting excitons can be realistic only at very low T ($\sim 0.15D$). We performed least square fitting of our heat-capacity and susceptibility data with the model between 2 and 18 K [see Figs. 4(b) and 5, respectively]. The fittings are found to be reasonably good both for C_{mag} and χ_{spin}^{\parallel} , particularly below 15 K. For C_{mag} , the best fit is observed for $D/J = -8.5$, while in case of χ_{spin}^{\parallel} we obtain $D/J = -9.1$. The D/J obtained from two different measurements are reasonably close and ensure the validity of the model used. We have extrapolated the low- T fitting curves to higher values of T for both C_{mag} and χ_{spin}^{\parallel} . The fitted curves deviate markedly above 20 K and fail to produce the broad peaklike feature present in the experimental data. This discrepancy is due to the fact that interaction be-

tween excitons is neglected in the present model.

In order to formulate a model which is applicable over the whole T range, Papanicolaou and Spathis extended their calculation by using direct strong coupling expansion of the free energy, which takes into account the interaction between excitons and is expected to be valid over a broad temperature range.^{29,30} The calculations provide the analytic expression of C_{exc} up to the third-order perturbation term and for χ_{exc} up to second order term (see Eqs. 3.20 and 4.25 in Ref. 29). The expressions for C_{exc} and χ_{exc}^{\parallel} are found to be fairly accurate as evident from their convergence to the other less rigorous models under specific approximations. However, the transverse susceptibility calculated in this model is found to be less reliable and the error for the second-order result is estimated to be about 6%.

Figures 4(b) and 5, respectively, show the fittings of C_{exc} and χ_{exc}^{\parallel} data (solid lines) between 2 and 100 K using formula derived from direct strong coupling expansion method. The fitted data reproduce our experimental result fairly well over a wide range of T . The model produces the peak in the data, which was lacking with the dilute exciton model. For C_{mag} , however, clear deviation is found above 75 K, which is presumably related to the uncertainty in calculating the lattice contribution at high- T . The value of the ratio $D/|J|$ is found to be close to 9 in the case of both heat capacity and the susceptibility fittings.

In the region $T > |J|$, it is expected that χ will be independent of H . Considering this fact, one can simulate $\Delta\sigma^{\parallel}(T)$ using the strong coupling relation of χ_{spin}^{\parallel} . The simulated data has been plotted along with the experimental $\Delta\sigma^{\parallel}(T)$ in the region $T > |J|$ [shown in Fig. 3(b)]. The simulated curve is found to match well at high- T side, but due to the dominating J , impurities, and broken-chain effects, it does not hold good in $T < |J|$ regime. This clearly indicates that spin excitation as predicted by the strong coupling expansion satisfactorily describes the MCE behavior at least above $T > |J|$ region.

It is to be noted that for few other anisotropic $S=1$ systems (such as NENP and NENC), there also exists in-plane (rhombic) anisotropy¹⁶ in addition to the planar anisotropy. In order to probe the existence of in-plane anisotropy, we measured χ along different directions in the ab plane, however, no anisotropy in χ (feature and/or magnitude) was observed. Therefore, we have not taken into account the contribution of in-plane anisotropy in the expressions of χ and C_{mag} for SNPO.

IV. SUMMARY AND CONCLUSION

So far the LD phase has been mostly observed and/or predicted in metal-organic complexes and metal halides. Therefore, the observation of such disordered magnetic phase in oxide material such as SNPO is unique. As discussed earlier, the parameter $D/|J|$ determines the low lying excitation in systems by Eq. (1). We found very consistent values of $D/|J|$ from our C and χ measurements. The quantity D/J has come out to be negative in all the analyses. Since D is established to be positive [from $\chi(T)$ data at high- T (Ref. 19)], J is certainly negative. This indicates an

AFM type intrachain interaction for SNPO. The measurements carried out on different sets of crystals also produce very similar values of the parameter. The consistency not only establishes the LD phase in SNPO, it also justifies the theoretical model proposed by Papanicolaou and Spathis in describing the low-lying excitation in the LD phase.²⁹

Few other important points of the present magnetic and calorimetric studies on this LD phase material can be summarized as follows: (a) the signature of spin-spin correlation has been predicted by the bifurcation below 30 K in the FC and ZFC susceptibilities measured perpendicular to the chain axis. Although the phenomenon has often been attributed to spin glass freezing, weak bifurcation (such as the present sample) is possible by the development of short range correlation pinned by some defects (here broken-chain or site disorder). The formation of a glassy magnetic phase for SNPO can be ruled out because we do not observe any frequency dispersion in the ac susceptibility measurement (not shown here). The short-range correlation in the sample is also supported by the observed peak in C_{mag} . (b) The calculation of spin-only component of χ^{\parallel} shows a low moment state in the chain direction, which is expected for a LD ground state (predominantly, $S_z^i=0$). The isothermal magnetization below 10 K also shows a low value of M ($0.007 \mu_B$ per f.u. at 2 K) along the chain direction. This low value of M (ideally expected to be zero) is due to the impurity moment, which is also evident from the Curie tail in the $\chi(T)$ data. (c) The flat region with almost constant value observed in χ_{spin}^{\parallel} below 10 K is a signature of the LD phase with finite $D/|J|$. Similar flat region is also present in $C_{mag}(T)$. Due to the presence of J along the chain direction, the low-lying excitation (from the $S_z=0$ ground state) always creates bound pair of spins ($\uparrow\downarrow$) with net moment zero. Therefore, we expect to see an effectively zero-moment state along the chain axis as long as $T \leq |J|$ (for SNPO $|J| \sim 10$ K). One should remember that the bound pair that exist below $T \leq |J|$, are characteristically different from dimers. Because, the pair formation and their propagation is a dynamic one, and $S_z=+1$ and -1 may not remain in adjacent lattice sites. (d) The T dependence of $\Delta\sigma$ along and perpendicular to the chain direction (particularly above 10 K) provides valuable information regarding spin anisotropy and its response to an external field. This can be a useful method in understanding the spin structure in the anisotropic spin-chain system. By careful observation one can see plateaulike region in $\Delta\sigma$ below 10 K which is similar to the χ_{spin}^{\parallel} and $C_{mag}(T)$. The magnetic entropy of the system remains insensitive to H as the bound pairs of spins created in some sites do not response much to the external H . As T increases, the bound spin pairs gradually dissociate and H can cause effective spin alignment resulting considerable value of $\Delta\sigma$. The good agreement between the simulated and the experimental $\Delta\sigma^{\parallel}$ at $T > |J|$ supports the role of spin excitation toward the observed T variation in magnetic entropy. (e) Although SNPO and SCPO have very similar crystal structure, the magnetic ground states and the spin excitations are drastically different in these two compounds. Unlike SNPO, SCPO does not show any obvious spin gap and it does have anisotropic magnetic behavior. This illustrates how the behavior of a spin-chain system can differ depending upon the presence of integer (Ni: $S=1$ in SNPO) or half-

TABLE I. The single ion anisotropy parameter (D), the intrachain exchange term (J), and corresponding $D/|J|$ ratio in various $S=1$ HAFM spin-chain systems. Here \dagger and \S denote the values obtained from susceptibility and heat-capacity measurements in the present work.

Sample	D (K)	J (K)	$D/ J $
NENP ^a	12	-47.5	0.25
NENC ^b	6	-0.8	7.5
DTN ^c	8.1	-1.7	4.7
CsFeBr ₃ ^d	30	-6.4	4.7
SNPO(χ) [†]	90.5	-9.9	9.1
SNPO(C) [§]	94.5	-11.1	8.5

^aReference 3.

^bReference 6.

^cReference 13.

^dReference 17.

integer (Cu: $S=\frac{1}{2}$ in SCPO) magnetic element.

In Table I we have compared several $S=1$ compositions with planar anisotropy, which includes both LD and Haldane phase compounds. The most commonly known material showing LD phase is the NENC. Similar to the presently studied SNPO, NENC also has chainlike structure with Ni ions along the chain. The alternating Ni ions have different crystallographic environments and one Ni ion stays in the high spin state ($S=1$), while the other in the low spin state ($S=0$), thereby effectively having a “-1-0-1-0-1-”-type chain. The spin chain in SNPO also consists alternating Ni and Pt ions with Pt in the low spin state ($S=0$), thereby constituting spin structure similar to NENC.

However, the anisotropy in SNPO is found to be much higher than NENC. The magnitude of D depends on the symmetry of the environment around the metal ion. In case of SNPO, oxygen atoms around Ni constitute trigonal prismatic environment, which is rather strongly distorted from an octahedral site. On the other hand the $S=1$ Ni ions in NENC occupy a slightly distorted octahedral site and the anisotropy is lower than SNPO.³¹ The magnetic properties of the LD phase depend upon the parameter $D/|J|$, and for NENC it is close to 7.5 (see Table I) as compared to ~ 9 for SNPO. However, since the individual magnitudes of D and J are much larger in case of SNPO, the subtle low-lying excitation due to the LD phase can be observed up to higher temperature ($T \sim J \sim 10$ K). This is in contrary to the case of NENC, where it is restricted to sub-Kelvin temperature range.

In conclusion, we identify exotic LD phase in case of the inorganic oxide SNPO. We observe remarkable agreement of the magnetic susceptibility and the heat-capacity data with the available theoretical models. This not only proves the LD phase in SNPO, it also strongly advocates the applicability of the models to the systems for integer spin systems with planar anisotropy. The present work also shows how the MCE behavior can be influenced by the anisotropic spin structure. All the measurements were performed down to 2 K and with maximum field of 50 kOe. It might be interesting to study the material at sub-Kelvin temperature to see the stability of

the LD phase. In addition, the effect of an external field equivalent to the strength of the anisotropy ($\mu_B H \sim D$) is worth investigating.

ACKNOWLEDGMENTS

The present work is supported by the grants received from DST, India (Grant No. SR/FTP/PS-23/2006). S.C. and D.J. wish to acknowledge CSIR, India. The authors thank the

Low Temperature & High Magnetic Field (LTHM) facilities at CSR, Indore (sponsored by DST) for heat-capacity measurements. The Centre for Advanced Material, IACS is also acknowledged for the characterization of crystals. E-mail correspondence with H.-J. Mikeska (Hannover, Germany) regarding LD phase has been quite useful. Lastly, S.M. would like to thank M. R. Lees (Warwick, U.K.) and V. Hardy (CRISMAT, Caen, France) for useful discussion regarding this interesting material.

*sspsm2@iacs.res.in

- ¹F. D. M. Haldane, *Phys. Rev. Lett.* **50**, 1153 (1983).
- ²I. Affleck, *J. Phys.: Condens. Matter* **1**, 3047 (1989).
- ³J. P. Renard, M. Verdaguer, L. P. Regnault, W. A. C. Erkelens, J. Rossat-Mignod, J. Ribas, W. G. Stirling, and C. Vettier, *J. Appl. Phys.* **63**, 3538 (1988).
- ⁴H. Tasaki, *Phys. Rev. Lett.* **66**, 798 (1991).
- ⁵H.-J. Mikeska and A. K. Kolezhuk, in *Quantum Magnetism*, Lecture Notes in Physics Vol. 645, edited by U. Schollwöck, J. Richter, D. J. J. Farnell, and R. F. Bishop (Springer-Verlag, Berlin, 2004), p. 1.
- ⁶M. Orendáč, A. Orendáčová, J. Černák, A. Feher, P. J. C. Signore, M. W. Meisel, S. Merah, and M. Verdaguer, *Phys. Rev. B* **52**, 3435 (1995).
- ⁷A. F. Albuquerque, C. J. Hamer, and J. Oitmaa, *Phys. Rev. B* **79**, 054412 (2009).
- ⁸N. Elstner and H.-J. Mikeska, *Z. Phys. B: Condens. Matter* **89**, 321 (1992).
- ⁹M. T. Batchelor, X.-W. Guan, and N. Oelkers, *Phys. Rev. B* **70**, 184408 (2004).
- ¹⁰W. Chen, K. Hida, and B. C. Sanctuary, *Phys. Rev. B* **67**, 104401 (2003).
- ¹¹Y. Hatsugai and M. Kohmoto, *Phys. Rev. B* **44**, 11789 (1991).
- ¹²A. Paduan-Filho, X. Gratens, and N. F. Oliveira, Jr., *Phys. Rev. B* **69**, 020405(R) (2004).
- ¹³V. S. Zapf, D. Zocco, B. R. Hansen, M. Jaime, N. Harrison, C. D. Batista, M. Kenzelmann, C. Niedermayer, A. Lacerda, and A. Paduan-Filho, *Phys. Rev. Lett.* **96**, 077204 (2006).
- ¹⁴S. A. Zvyagin, J. Wosnitzer, C. D. Batista, M. Tsukamoto, N. Kawashima, J. Krzystek, V. S. Zapf, M. Jaime, N. F. Oliveira, Jr., and A. Paduan-Filho, *Phys. Rev. Lett.* **98**, 047205 (2007).
- ¹⁵S. A. Zvyagin, T. Rieth, M. Sieling, S. Schmidt, and B. Lüthi, *Czech. J. Phys.* **46**, 1937 (1996).
- ¹⁶M. Orendáč, S. Zvyagin, A. Orendáčová, M. Seiling, B. Lüthi, A. Feher, and M. W. Meisel, *Phys. Rev. B* **60**, 4170 (1999).
- ¹⁷B. Dorner, D. Visser, U. Steigenberger, K. Kakurai, and M. Steiner, *Physica B* **156&157**, 263 (1989).
- ¹⁸M. Orendáč, E. Čížmár, A. Orendáčová, J. Černák, A. Feher, M. W. Meisel, K. A. Abboud, S. Zvyagin, M. Sieling, T. Rieth, and B. Lüthi, *Phys. Rev. B* **61**, 3223 (2000).
- ¹⁹J. B. Claridge, R. C. Layland, W. H. Henley, and H.-C. zur Loye, *Chem. Mater.* **11**, 1376 (1999).
- ²⁰T. N. Nguyen, D. M. Giaquinta, and H.-C. zur Loye, *Chem. Mater.* **6**, 1642 (1994).
- ²¹N. Mohapatra, K. K. Iyer, S. Rayaprol, and E. V. Sampathkumaran, *Phys. Rev. B* **75**, 214422 (2007).
- ²²Y. Liu, J. E. Drumheller, and R. D. Willett, *Phys. Rev. B* **52**, 15327 (1995).
- ²³S. Majumdar, V. Hardy, M. R. Lees, D. McK. Paul, H. Rous-selière, and D. Grebille, *Phys. Rev. B* **69**, 024405 (2004).
- ²⁴R. L. Carlin, C. J. O. Connor, and S. N. Bhatia, *J. Am. Chem. Soc.* **98**, 3523 (1976).
- ²⁵O. Kahn, *Molecular Magnetism* (VCH, New York, 1993), pp. 17–20.
- ²⁶M. Bouvier, P. Lethuillier, and D. Schmitt, *Phys. Rev. B* **43**, 13137 (1991).
- ²⁷N. Papanicolaou and P. Spathis, *J. Phys.: Condens. Matter* **1**, 5555 (1989).
- ²⁸N. Papanicolaou and P. Spathis, *J. Phys.: Condens. Matter* **2**, 6575 (1990).
- ²⁹N. Papanicolaou and P. N. Spathis, *Phys. Rev. B* **52**, 16001 (1995).
- ³⁰A. Orendáčová, M. Orendáč, A. Feher, M. W. Meisel, P. J. C. Signore, S. Merah, and M. Verdaguer, *Czech. J. Phys.* **46**, 1939 (1996).
- ³¹J. Černák, J. Chomič, D. Baloghová, and M. Dunaj-Jurčo, *Acta Crystallogr., Sect. C: Cryst. Struct. Commun.* **44**, 1902 (1988).